Lipids in Health and Disease

RESEARCH

Open Access

Arachidonic acid suppresses lung cancer cell growth and modulates lipid metabolism and the ERK/PPARγ signaling pathway

Lin Wang[1], Lanlan Wei[1], Xueling Chen[2] and Jiali Xiong[1*]

Abstract

Lung cancer remains the leading cause of cancer-related mortality worldwide, necessitating the development of new treatment strategies. Arachidonic acid (ARA), a polyunsaturated fatty acid, shows promise in cancer therapy due to its potential anti-tumor effects, although its role in lung cancer remains unclear. This study investigated the effects and underlying mechanism of ARA on A549 and NCI-H1299 lung cancer cells. In vitro assays were used to assess cell viability, apoptosis, colony formation, lipid droplet formation, and changes in cellular lipid content. ARA dose-dependently suppressed cell viability, facilitated apoptosis, and suppressed colony formation in both lung cancer cell lines. Network pharmacology analysis was performed to identify potential gene targets and pathways, uncovering 61 overlapping genes between ARA and lung cancer-related targets, with mitogen-activated protein kinase 1 (MAPK1) emerging as a key gene. Enrichment analyses suggested that the effects of ARA might be mediated through lipid metabolism and the extracellular signal-regulated kinase (ERK)/peroxisome proliferator-activated receptor gamma (PPARγ) signaling pathway. In both lung cancer cell lines, ARA treatment inhibited lipid droplet formation and decreased the cellular lipids. Immunoblotting further confirmed that ARA treatment significantly increased ERK phosphorylation while reducing PPARγ and fatty acid synthase (FASN) protein levels. In vitro experiments using GW9662, a PPARγ antagonist, confirmed that inhibiting lipid droplet formation impairs lung cancer cell viability and promotes apoptosis. Furthermore, in vivo experiments demonstrated that ARA significantly reduced tumor size and weight in a lung cancer xenograft model, further validating its anti-tumor effects. The potential of ARA as a therapeutic agent for lung cancer might involve lipid metabolism and relevant signaling pathways. A future study exploring the full therapeutic potential of ARA and underlying mechanisms in lung cancer is needed.

Keywords Arachidonic acid (ARA), Lung cancer, The extracellular signal-regulated kinase (ERK)/peroxisome proliferator-activated receptor gamma (PPARγ) pathway, Lipid metabolism, Mitogen-activated protein kinase 1 (MAPK1)

*Correspondence:
Jiali Xiong
18673371226@163.com
[1]Department of Respiratory and Critical Care Medicine, Zhuzhou Central Hospital, ZhuZhou 412000, Hunan Province, China
[2]Emergency Center, Zhuzhou Central Hospital, ZhuZhou 412000, Hunan Province, China

Introduction

In 2022, lung cancer continued to be the most common cancer diagnosed worldwide, with around 2.5 million new cases, or one in eight malignancies, making it the leading cause of cancer-related death worldwide [1]. The overall survival rate for patients with lung cancer is still low, despite advancements in medical therapies, especially for those with advanced-stage disease [2].

Currently, surgery, chemotherapy, radiation, and targeted therapies are the main treatments for lung cancer [3]. Regarding non-small cell lung cancer (NSCLC), which makes up around 85% of instances of lung cancer, first-line treatment commonly involves platinum-based chemotherapy agents, such as cisplatin or carboplatin [4, 5]. Additionally, individuals with particular genetic alterations, like epidermal growth factor receptor (EGFR) or anaplastic lymphoma kinase (ALK) mutations, now require targeted therapy, such as tyrosine kinase inhibitors (TKIs) like gefitinib, erlotinib, and osimertinib [6, 7]. However, despite these advances, the limitations and side effects of these treatments present significant challenges. Chemotherapy is often associated with severe systemic toxicity, leading to complications such as nephrotoxicity, neurotoxicity, and myelosuppression, significantly affecting patients' quality of life [8]. Resistance to TKIs develops over time in many patients, rendering the treatment less effective and leading to disease progression [9, 10]. The effectiveness of immunotherapies, including immune checkpoint inhibitors like pembrolizumab, is confined to specific patient subgroups and frequently comes with immune-related adverse events, such as pneumonitis and colitis [11, 12]. Given the limitations of current therapies, the development of novel therapeutic agents with improved efficacy and a reduced side-effect profile is essential.

Arachidonic acid (ARA), a polyunsaturated fatty acid, plays a vital role as a key component of cellular membranes, contributing to the fluidity and flexibility necessary for normal cellular functions. This role is especially important in tissues such as the nervous system, skeletal muscle, and immune system [13]. Recent studies indicate that ARA may possess anti-tumor properties. ARA has been shown to selectively induce tumor cell death in vitro by initiating lipid peroxidation at the cell membrane, an effect reversible with antioxidants such as vitamin E, uric acid, glutathione peroxidase, and superoxide dismutase [14, 15]. Reportedly, lipid peroxidation inhibitors have been shown in vitro to repair the cell death caused by ARA in multiple myeloma cell lines [14, 16]. In addition, free ARA has displayed cytotoxic activity against both vincristine-sensitive (KB-3-1) and vincristine-resistant (KB-Ch(R)-8-5) cancer cells in vitro, likely through a mechanism reliant on free radical formation [17]. Despite these previous studies, its role and precise mechanisms in lung cancer need further in-depth exploration.

This study seeks to explore the anti-tumor properties of ARA in lung cancer, particularly examining its downstream molecular targets. The impact of ARA on various lung cancer cell phenotypes was assessed in vitro. Network pharmacology analysis, coupled with experimental validation, was used to pinpoint key gene targets and signaling pathways linked to the therapeutic effects of ARA. Additionally, the study investigated the specific influence of ARA on lipid metabolism within lung cancer cells. By integrating these findings with experimental data, this study seeks to uncover the signaling mechanisms modulated by ARA, providing a basis for its development as a potential therapeutic agent in lung cancer treatment.

Materials and methods

Cell culture and treatment

Lung cancer cells A549 and NCI-H1299 were obtained from Cell Bank/Stem Cell Bank (Chinese Academy of Sciences, Beijing, China) and cultivated in Dulbecco's Modified Eagle Medium (DMEM; Gibco, 11960044 Grand Island, NY, USA) enhanced with 1% penicillin-streptomycin (Gibco) and 10% fetal bovine serum (FBS; A5256701 Gibco). The cells were kept in a humidified environment with 5% CO_2 at 37 °C. ARA (CAS No.:506-32-1; A9673, Sigma-Aldrich, St. Louis, MO, USA) was dissolved in ethanol and used at concentrations of 10, 25, 50, and 100 μM [18, 19]. Cells were treated with ARA for 24, 48, and 72 h for various assays [18, 19].

Cell viability assay

Cell viability was evaluated utilizing the CCK-8 assay. A549 and NCI-H1299 cells were plated in 96-well plates at a density of 5,000 cells per well and treated with 25, 50, and 100 μM ARA for durations of 24, 48, and 72 h. Following the treatment period, CCK-8 (10 μL; CK04, Dojindo, Kumamoto, Japan) was introduced to each well, and the samples were incubated for 2 h at 37 °C. Absorbance was quantified at 450 nm utilizing a microplate reader (Bio-Rad, Hercules, CA, USA). Regarding GW9662 treatment, cells were treated with 40 μM GW9662 for 48 h and applied to CCK-8 assay as described.

Trypan blue exclusion assay

Cell death was evaluated using the trypan blue exclusion assay. A549 and NCI-H1299 cells underwent treatment with ARA at concentrations of 25 and 50 μM for a duration of 48 h. Post-treatment, cells were collected and stained using trypan blue solution (0.4%; T8154, Sigma-Aldrich). Cells, both viable and non-viable, were enumerated utilizing a hemocytometer and observed under a light microscope (Olympus, Tokyo, Japan). By dividing

the number of trypan blue-positive cells by the total number of cells, the percentage of cell death was calculated. Regarding GW9662 treatment, cells were treated with 40 μM GW9662 for 48 h and applied to Trypan blue exclusion assay as described.

Colony formation assay

Lung cancer cell growth after ARA treatment was assessed by measuring colony formation. Six-well plates were used to plate A549 and NCI-H1299 cells at a density of 500 cells per well. After adhering overnight, the cells were treated with 10 and 25 μM ARA and incubated for 10–14 days, allowing colonies to form. After 15 min of paraformaldehyde (4%; P1110; Solarb) fixation, cells were stained for 20 min with crystal violet (C0121; Beyotime). Colonies including over 50 cells were enumerated using a microscope.

Flow cytometry assay

Apoptosis was analyzed using an Annexin V-FITC/PI apoptosis detection kit (BD Biosciences, San Jose, CA, USA) following the manufacturer's instructions. A549 and NCI-H1299 cells were treated with ARA at the concentrations of 25 μM for 48 h. After treatment, cells were harvested, washed twice with cold PBS, and resuspended in 1× binding buffer. Subsequently, cells were incubated with 5 μL of Annexin V-FITC and 5 μL of propidium iodide (PI) for 15 min in the dark at room temperature. Stained cells were immediately analyzed using a flow cytometer (FACSCalibur, BD Biosciences), and data were processed using FlowJo software (BD Biosciences). Apoptotic cells were categorized as early apoptosis (Annexin V-FITC positive, PI negative) or late apoptosis (Annexin V-FITC and PI double positive). Each experiment was performed in triplicate. Regarding GW9662 treatment, cells were treated with 40 μM GW9662 for 48 h and applied to Flow cytometry assay as described.

Network pharmacology analysis

Molecular targets of ARA in lung cancer were identified via network pharmacology. Target genes associated with ARA were sourced from the Comparative Toxicogenomics Database (CTD) (https://ctdbase.org/), STITCH [20], SwissTargetPrediction [21], and the Traditional Chinese Medicine Systems Pharmacology Database and Analysis Platform (TCMSP; https://old.tcmsp-e.com/tcmsp.php) [22]. Genes associated with lung cancer were sourced from the GeneCards database (https://www.genecards.org/). An analysis of the intersection of ARA-related genes and lung cancer-related genes was performed to identify overlapping disease and therapeutic target genes. The protein-protein interaction (PPI) network for these genes was established utilizing the STRING database (https://string-db.org/), and module analysis was conducted employing Cytoscape software with the MCODE plugin (https://cytoscape.org/). To determine the biological processes and pathways enriched among the target genes, Kyoto Encyclopedia of Genes and Genomes (KEGG) pathway analysis and Gene Ontology (GO) enrichment analysis were conducted.

Oil red O staining

Using oil red O staining, the production of lipid droplets in A549 and NCI-H1299 cells treated with ARA was assessed. The cells underwent a 48-hour treatment with 25 μM ARA, a 15-minute fixation period in 4% paraformaldehyde, and a 30-minute staining period with oil red O solution (G1262; Solarbi). At the end of the staining, cells were washed with distilled water, and the number of lipid droplets was quantified under a microscope.

Nile red staining

Nile red staining was utilized to visualize and quantify cellular lipid content in A549 and NCI-H1299 cells after treatment with 25 μM ARA. Following 48-hour ARA treatment, cells were stained with Nile red solution (G1264; Solarbi) for 10 min in the dark. Cells were washed with PBS, and images were captured using a fluorescence microscope (Carl Zeiss, Oberkochen, Germany). Quantification of Nile red staining intensity was performed using ImageJ software, providing an index of cellular lipid content.

Immunoblotting

Immunoblotting was performed to assess the levels of key proteins involved in the extracellular signal-regulated kinase (ERK)/peroxisome proliferator-activated receptor gamma (PPARγ) pathway. A549 and NCI-H1299 cells underwent treatment with ARA for a duration of 48 h. Post-treatment, cells were lysed utilizing RIPA buffer (Sigma-Aldrich) augmented with protease and phosphatase inhibitors (P5726, Sigma-Aldrich). Protein quantities were quantified by the BCA assay (Thermo Fisher Scientific, Waltham, MA, USA). Identical quantities of protein (30 μg) were fractionated via SDS-PAGE and subsequently transferred to PVDF membranes (Millipore, IPVH00010; Burlington, MA, USA). After being exposed to 5% non-fat milk for an hour, the membranes were incubated with primary antibodies targeting ERK (9102, Cell Signaling, Danvers, MA, USA), PPARγ (2443, Cell Signaling), and fatty acid synthase (FASN) (sc-55580, Santa Cruz Biotechnology, Dallas, TX, USA) for the entire night at 4 °C. Membranes were cleaned and then treated for an hour with HRP-conjugated secondary antibodies (7074, Cell Signaling). An improved chemiluminescence kit (34580, Thermo Fisher Scientific) was used to identify the protein bands, and ImageJ software was used to quantify the results.

In vivo tumor xenograft model

Nude mice (4–6 weeks old, male, weighing 18–22 g) were obtained from Guangdong Medical Laboratory Animal Center and housed under specific pathogen-free (SPF) conditions. All experimental protocols were approved by the the Guangdong Medical Laboratory Animal Center Ethical Committee. NCI-H1299 cells (1×10^7 cells in 100 µL PBS) were subcutaneously injected into the right flank of the mice. When tumors reached a volume of 100–200 mm^3, mice were randomly assigned to either the control group or the ARA-treated group ($n = 5$ per group). The ARA-treated group received intraperitoneal injections of 2 mg/kg ARA every 3 days for 3 weeks, while the control group received vehicle solution under the same schedule. Tumor size was measured using calipers every 3 days, and tumor volume was calculated using the formula:

$$\text{Tumor volume} = \frac{1}{2} \times length \times width^2$$

At the end of the treatment period, tumors were excised, weighed, and subjected to immunoblotting analysis as described above.

Statistical analysis

Four duplicates of each experiment were conducted, and the results were reported as mean ± SD. The Mann-Whitney rank sum test followed by Bonferroni correction was applied to evaluate the significant differences. A *P*-value below 0.05 was considered statistically significant. GraphPad Prism (version X.0, GraphPad Software, San Diego, CA, USA) was used for all statistical analyses.

Results

Anti-tumor effect of ARA in A549 and NCI-H1299 lung cancer cells

Compared to the control group, ARA treatment at concentrations of 25, 50 and 100 µM significantly reduced cell viability after 48 and 72 h, as shown by the CCK-8 assay (Fig. 1A; $P < 0.05$). ARA also induced significant cell death in a dose-dependent manner, as shown by the trypan blue exclusion assay, with a significantly higher proportion of non-viable cells in the 525 and 50 µM treatment groups after 48 h compared to untreated cells (Fig. 1B; $P < 0.05$). Additionally, compared to the control group, the colony formation ability of both cell lines was markedly reduced after treatment with 10 and 25 µM ARA (Fig. 1C; $P < 0.05$). Furthermore, compared to the control group, 25µM ARA treatment significantly facilitated cell apoptosis in both lung cancer cell lines (Fig. 1D; $P < 0.05$).

Network pharmacology analysis of ARA in lung cancer

After confirming the in vitro anti-tumor effects of ARA in lung cancer cells, an integrative bioinformatics analysis was performed to identify its potential downstream target(s). An initial screening was conducted through network pharmacology analysis. Using the CTD, STITCH, SwissTargetPrediction, and TCMSP databases, 85 genes associated with ARA were identified as drug targets. Lung cancer-related genes were retrieved from the GeneCards database and a total of 3400 genes were identified as disease targets; the intersection between ARA-related and lung cancer-related genes resulted in 61 common genes as disease/drug targets (Fig. 2A). The genes were subsequently entered into the STRING database to create a PPI network. The PPI network underwent additional analysis utilizing the MCODE plugin within Cytoscape software, which divided the network into modules and assigned scores. Compared to other genes, mitogen-activated protein kinase 1 (MAPK1), which encodes the ERK protein, was identified as the top hub gene with the highest MCODE score (Fig. 2B), indicated by the red color and larger circle size, signifying a higher degree of connectivity. GO and KEGG enrichment analyses were performed on the overlapping genes, with GO analysis yielding response to inorganic substance, response to oxidative stress, response to reactive oxygen species, and so on and ranking the sixth pathway as lipid metabolism-related (Fig. 2C), while KEGG analysis showed the top pathway also related to lipid metabolism (Fig. 2D). This suggests that ARA might exert its anti-tumor effects in lung cancer through the modulation of MAPK1 and lipid metabolism pathways.

ARA inhibits lipid droplet formation in lung cancer cells

Next, the specific effects of ARA on lipid metabolism were investigated. Oil red O staining was performed on A549 cells and NCI H1299 cells treated with 25µM ARA. Figure 3A shows that ARA significantly inhibited the lipid droplet formation in lung cancer cell lines compared to the control group. In addition, Nile red staining of cellular lipids in A549 cells and NCI H1299 cells shows that ARA treatment significantly decreased the cellular lipids in both cell lines compared to the control group (Fig. 3B).

Lipid droplet formation inhibitor suppresses lung cancer cell malignancy

To further investigate the role of lipid droplet formation in lung cancer cell malignancy, A549 and NCI H1299 cells were treated with 40 µM GW9662 and examined for cell phenotypes. Figure 4A-B shows that GW9662 significantly inhibited cell viability of both cell lines. Consistently, GW9662 remarkably facilitated cell death and cell apoptosis, as revealed by Trypan blue exclusion assay and Flow cytometry (Fig. 4C-F).

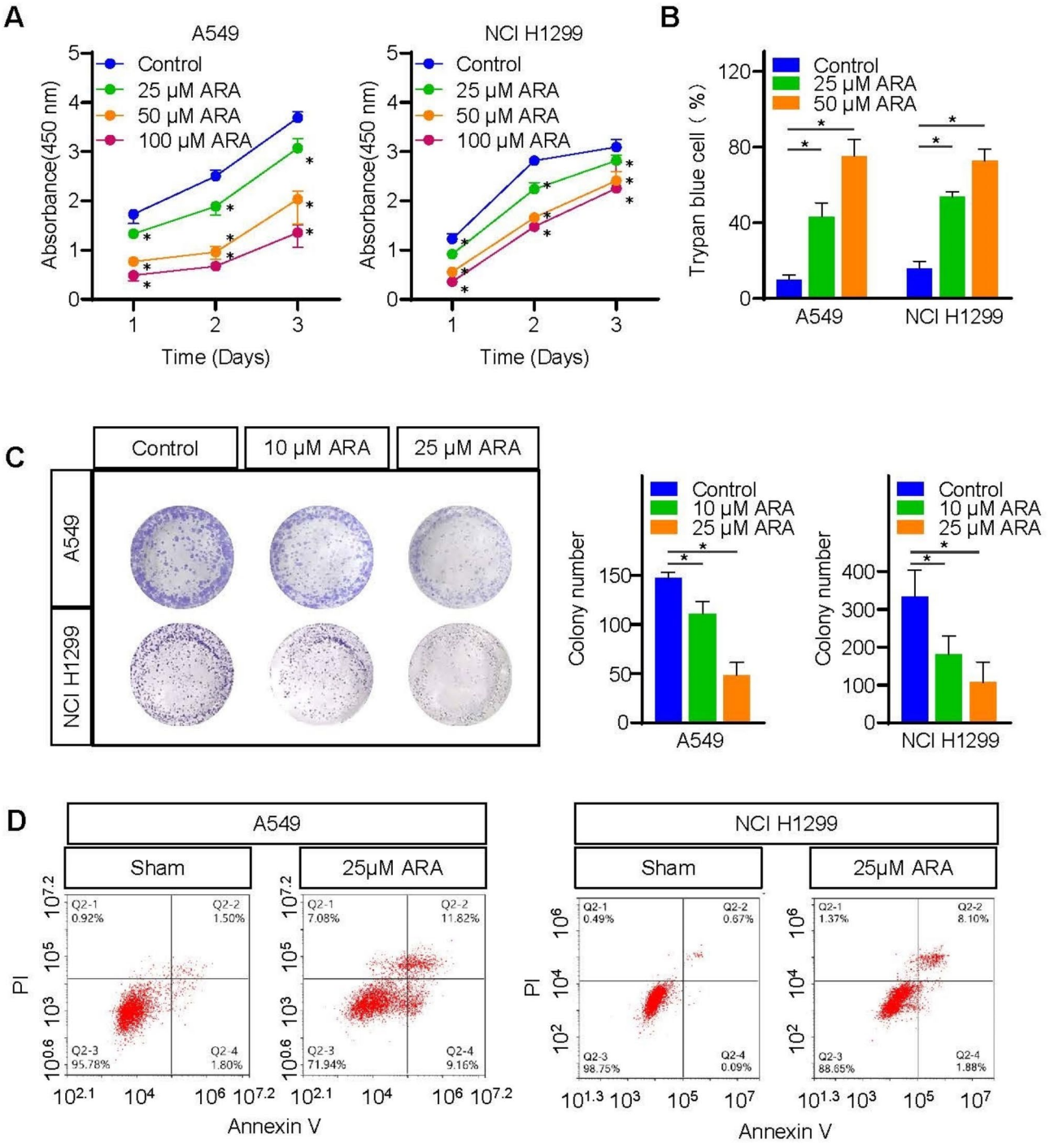

Fig. 1 Anti-tumor effect of Arachidonic Acid (ARA) in A549 and NCI-H1299 lung cancer cells. Two lung cancer cell lines, A549 and NCI-H1299 were treated with 10, 25, 50, or 100 μM ARA for 24, 48, or 72 h. (**A**) CCK-8 assay was performed to detect cell viability. (**B**) Trypan blue exclusion assay was performed to detect cell death. (**C**) Colony formation assay was performed to detect proliferative capacity. (**D**) Flow cytometry assay was performed to detect cell apoptosis. Cells Data are presented as means ± SD of four independent experiments. Statistical analyses were conducted using the Mann-Whitney U test with Bonferroni correction. Statistical significance: **P* < 0.05 compared to control groups

Effect of ARA on the ERK/PPARγ pathway in A549 and NCI-H1299 cells

Immunoblotting analysis showed that, compared to control cells, ARA treatment led to a significant increase in ERK phosphorylation and a reduction in PPARγ and FASN levels in both A549 and NCI-H1299 cells after 48 h (Fig. 5A-B; $P < 0.05$). These findings indicate that ARA might exert its anti-tumor effects by modulating

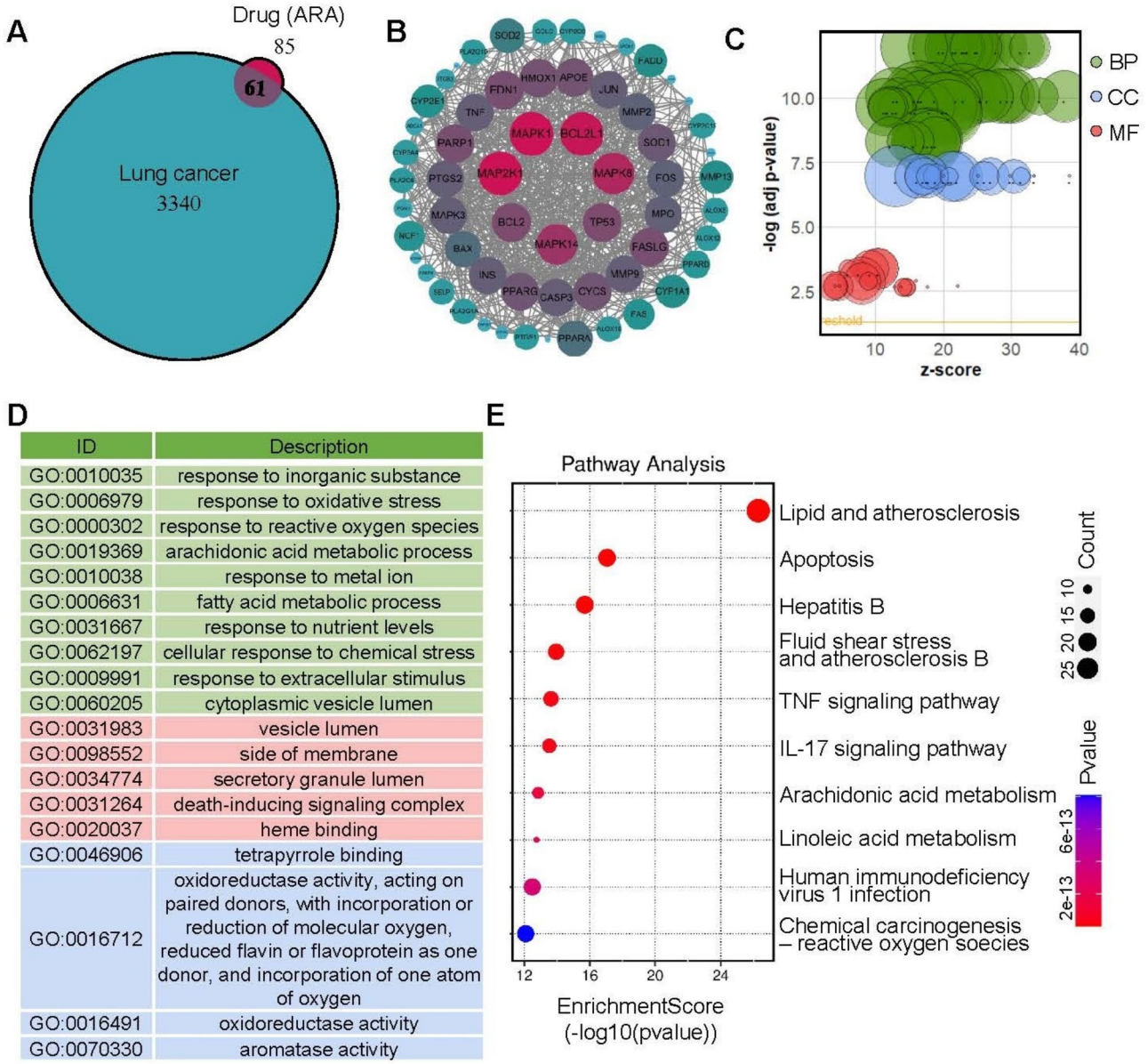

ID	Description
GO:0010035	response to inorganic substance
GO:0006979	response to oxidative stress
GO:0000302	response to reactive oxygen species
GO:0019369	arachidonic acid metabolic process
GO:0010038	response to metal ion
GO:0006631	fatty acid metabolic process
GO:0031667	response to nutrient levels
GO:0062197	cellular response to chemical stress
GO:0009991	response to extracellular stimulus
GO:0060205	cytoplasmic vesicle lumen
GO:0031983	vesicle lumen
GO:0098552	side of membrane
GO:0034774	secretory granule lumen
GO:0031264	death-inducing signaling complex
GO:0020037	heme binding
GO:0046906	tetrapyrrole binding
GO:0016712	oxidoreductase activity, acting on paired donors, with incorporation or reduction of molecular oxygen, reduced flavin or flavoprotein as one donor, and incorporation of one atom of oxygen
GO:0016491	oxidoreductase activity
GO:0070330	aromatase activity

Fig. 2 Network pharmacology analysis of ARA in lung cancer. (**A**) Venn diagram showing the intersection of ARA-targeted and lung cancer-targeted genes. (**B**) Protein-protein interaction (PPI) network of potential targets, where red indicates primary proteins, and the size of the targets corresponds to their degree value. (**C-D**) Gene Ontology (GO) enrichment analysis of the potential target PPI network, with green representing biological processes (BP), blue representing cellular components (CC), and red representing molecular functions (MF). (**E**) KEGG pathway enrichment analysis of the potential target PPI network

the ERK/PPARγ signaling pathway and inhibiting lipid metabolism in lung cancer cells.

ARA inhibits tumor growth and modulates the ERK/PPARγ signaling pathway in a lung cancer mouse model

To evaluate the in vivo anti-tumor effects of ARA, a lung cancer mouse xenograft model was established by subcutaneously injecting NCI-H1299 cells into nude mice. When tumors reached a volume of 100–200 mm^3, mice were treated with either ARA (2 mg/kg) or vehicle solution via intraperitoneal injection every 3 days for 3 weeks. Representative images of the excised tumors illustrate the reduction in tumor size in the ARA-treated group; as shown in Fig. 6A, ARA treatment remarkably decreased tumor volumes. Compared to the control group, ARA treatment significantly reduced tumor weight (Fig. 6B; $P < 0.05$).

To investigate whether ARA exerts in vivo anti-tumor effects through the ERK/PPARγ signaling pathway, immunoblotting was performed on tumor samples. ARA treatment led to a significant increase in ERK phosphorylation and a concomitant decrease in PPARγ and FASN

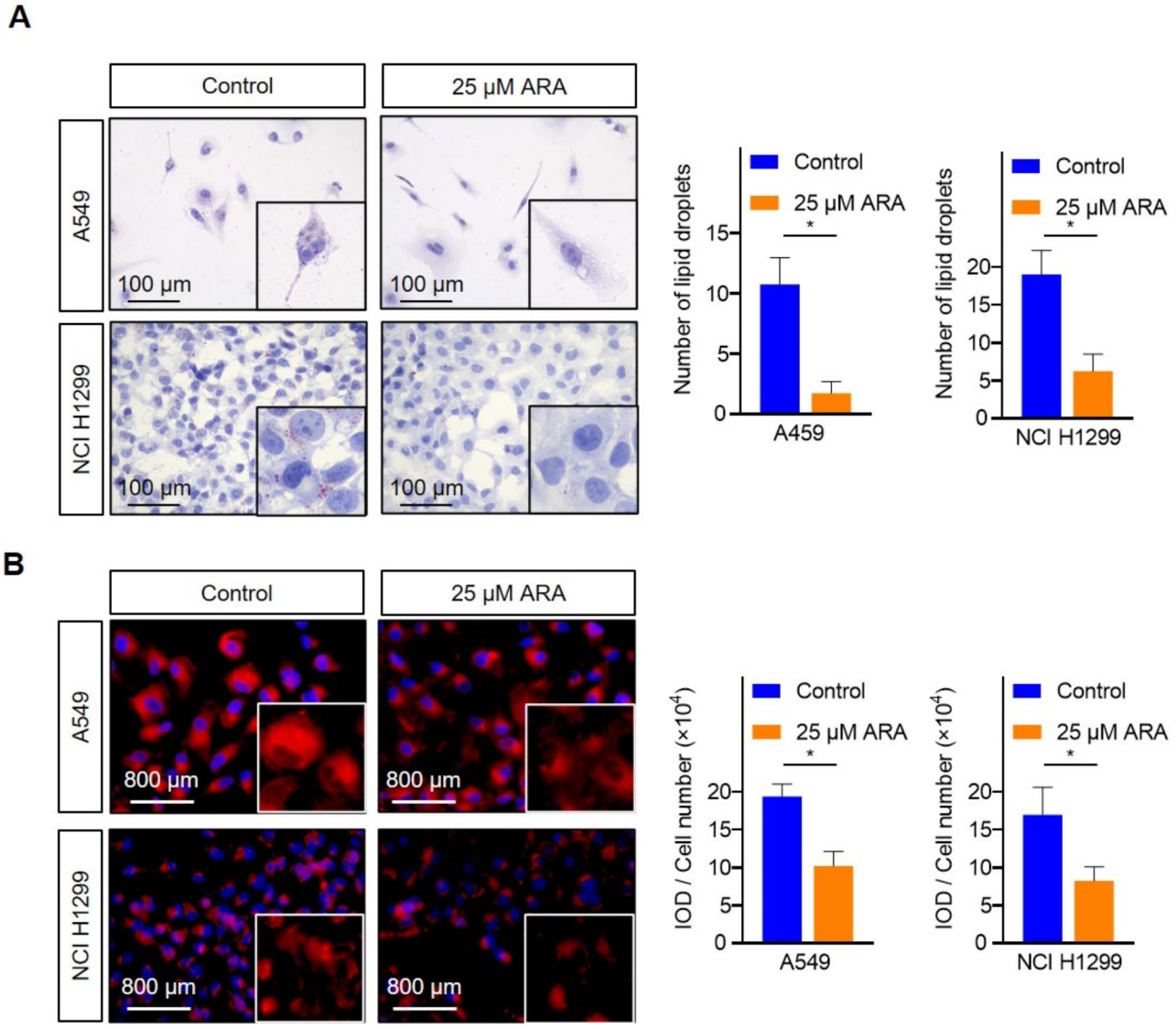

Fig. 3 ARA inhibits lipid droplet formation in lung cancer cells. (**A**) Oil red O staining of A549 cells and NCI H1299 cells treated with 25μM ARA. Quantification of oil red O staining was performed to assess the number of lipid droplets. (**B**) Nile red staining of cellular lipids in A549 cells and NCI H1299 cells treated with 25μM ARA. Quantification of nile red staining was performed using image J software. Data are presented as the means ± SD (error bars) from four independent experiments. Statistical analyses were conducted using the Mann-Whitney U test with Bonferroni correction. **P* < 0.05 compared with control groups

protein levels compared to the control group (Fig. 6C; $P < 0.05$). These results suggest that ARA inhibits tumor growth by modulating the ERK/PPARγ signaling pathway and lipid metabolism in vivo.

Discussion

In this study, we demonstrate that ARA exhibits significant anti-tumor effects in A549 and NCI-H1299 lung cancer cells by dose-dependently suppressing cell viability, inducing cell death, inhibiting colony formation, and promoting cell apoptosis. Network pharmacology analysis identified 61 common ARA-related and lung cancer-related genes, with MAPK1 emerging as the top hub gene. GO and KEGG enrichment analyses revealed a strong association with lipid metabolism pathways, suggesting that ARA might exert its anti-tumor effects through modulation of lipid metabolism. Indeed, in both lung cancer cell lines, ARA treatment inhibited lipid droplet formation and decreased the cellular lipids. Immunoblotting analysis further confirmed that ARA treatment significantly increased ERK phosphorylation while reducing PPARγ and FASN levels, indicating that ARA might inhibit lipid metabolism through the ERK/PPARγ signaling pathway.

The ARA pathway, a critical metabolic process, has a significant role in carcinogenesis [23]. Cancer initiation

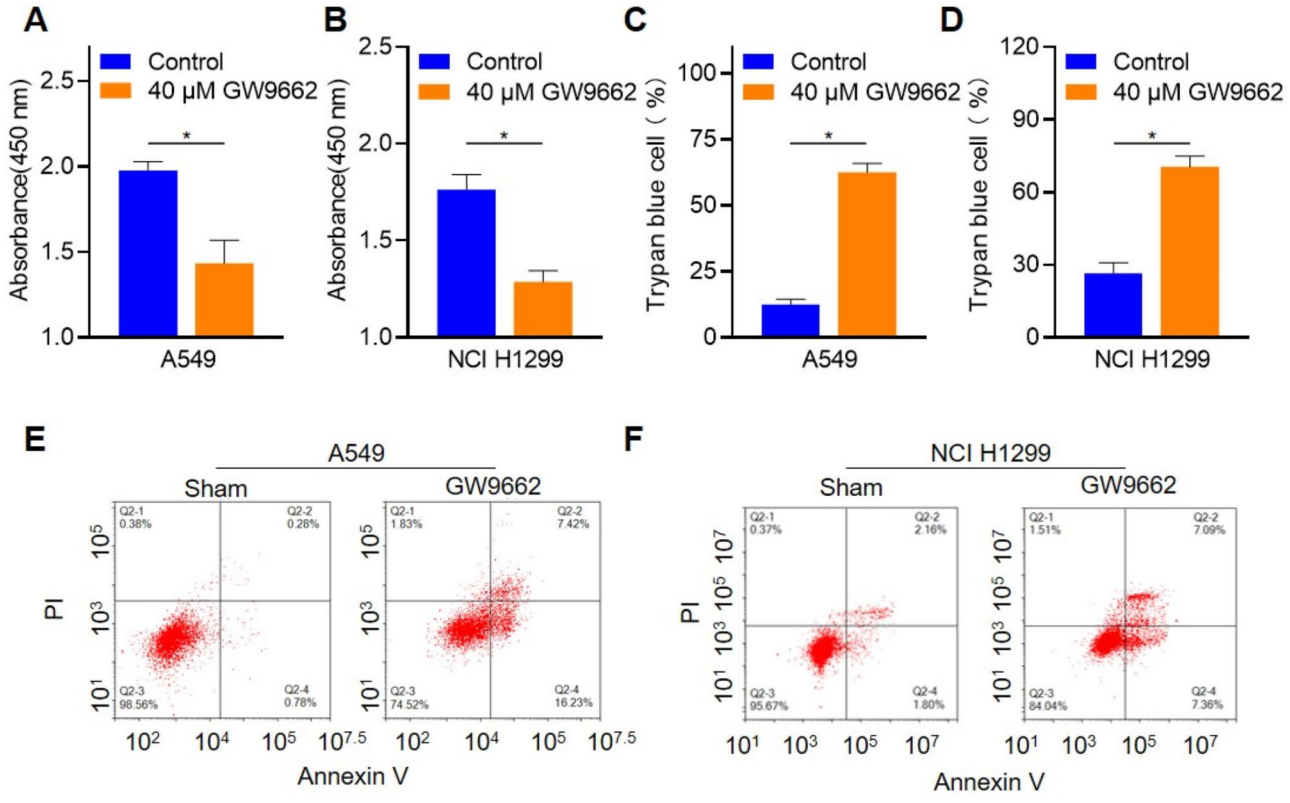

Fig. 4 Lipid droplet formation inhibitor suppresses lung cancer cell malignancy. A549 and NCI H1299 cells were treated with 40 μM GW9662 and examined for (**A-B**) cell viability using CCK-8 assay; (**C-D**) cell death using Trypan blue exclusion assay; (**E-F**) cell apoptosis using Flow cytometry. Cells Data are presented as means ± SD of four independent experiments. Statistical analyses were conducted using the Mann-Whitney U test with Bonferroni correction. Statistical significance: $^{*}P < 0.05$ compared to control groups

and progression are complex, multistep events regulated by various internal elements, such as growth factors and their receptors, cytokines, chemokines, transcription factors, nuclear receptors, and lipid mediators derived from ARA [24–27]. Although the role of ARA has been reported in several cancers, its specific functions and mechanisms in lung cancer are not fully understood. The initial assessment of the anti-tumor effects of ARA was designed to evaluate its impact on critical cellular behaviors associated with cancer progression, namely, proliferation, survival, and long-term reproductive potential [28, 29]. The observed dose-dependent inhibition of cell growth and increase in cell death, as well as promoted cell apoptosis suggest that ARA effectively disrupts essential mechanisms required for lung cancer cell survival. The reduction in colony formation further indicates that ARA not only affects immediate cellular functions but also impairs the long-term viability of cancer cells, which is critical for tumor progression [30].

Following confirmation of the anti-tumor effects of ARA in vitro, network pharmacology was employed to explore the molecular mechanisms underlying these effects. MAPK1 was identified as the top hub gene, underscoring its central role in the potential mechanisms of ARA action. MAPK1 encodes the ERK protein, a key regulator of cellular processes such as proliferation, differentiation, and survival [31–33]. The analysis also highlighted lipid metabolism pathways, essential for cancer development as cancer cells rely on large lipid quantities for energy, rapid growth, and membrane synthesis [34, 35]. Several existing chemotherapeutic agents affect lipid metabolism, and numerous drugs targeting lipid metabolism in cancer are currently under investigation and development [36]. As an SCD1 inhibitor, ginsenoside protopanaxatriol (g-PPT) has been shown to reduce polyunsaturated fatty acid production, inhibit triglyceride synthesis, and prevent lipid droplet accumulation in cancer cells. In non-small cell lung cancer cells resistant to TKIs, combining g-PPT with gefitinib successfully overcame drug resistance, inducing apoptosis and improving the therapeutic response [37]. Indeed, in both lung cancer cell lines, A549 and NCI-H1299, ARA treatment significantly inhibited lipid droplet formation and decreased cellular lipids, suggesting that ARA might exert its anti-tumor effects through modulation of lipid metabolism. To further investigate the contribution of lipid droplet formation to lung cancer cell malignancy, GW9662, a well-characterized PPARγ antagonist

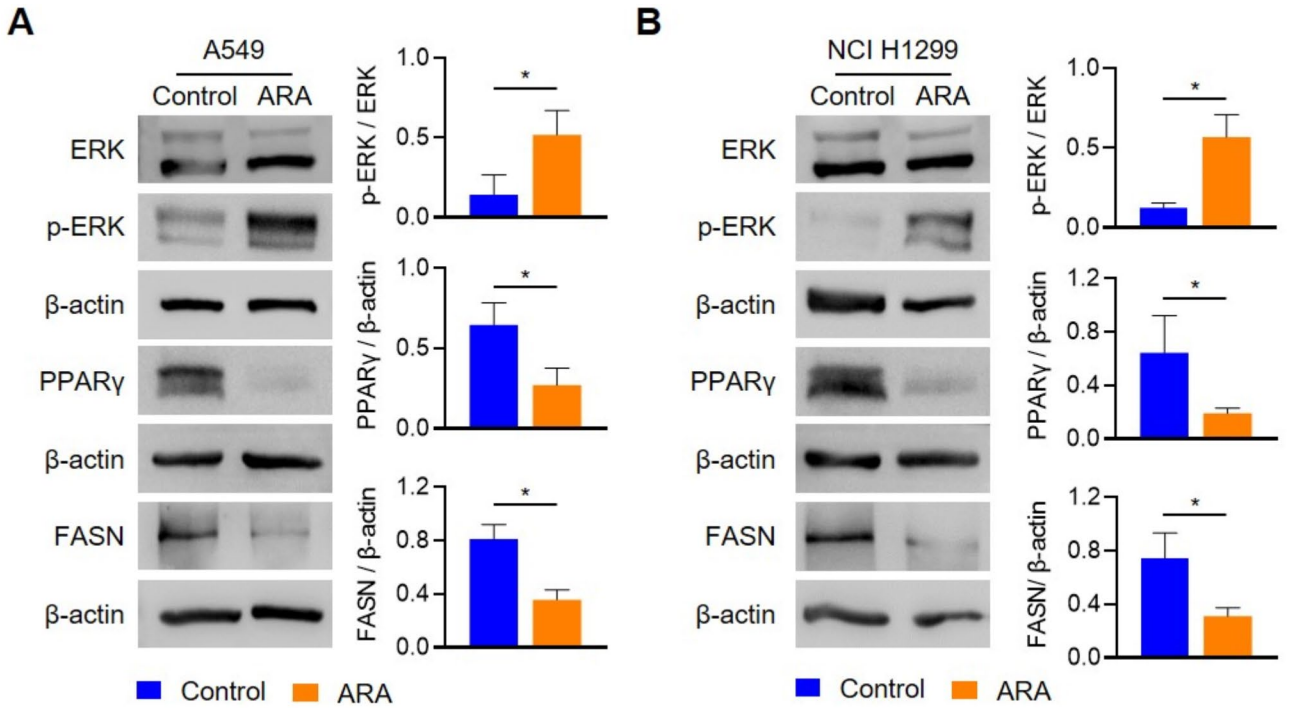

Fig. 5 Effect of ARA on the ERK/PPARγ pathway in A549 and NCI-H1299 cells. (**A**) Immunoblotting analysis of ERK, PPARγ, and FASN protein levels in A549 cells treated with 25 μM ARA for 48 h. (**B**) Immunoblotting analysis of ERK, PPARγ, and FASN protein levels in NCI H1299 cells treated with ARA for 48 h. Data are presented as means ± SD from four independent experiments. Statistical analyses were conducted using the Mann-Whitney U test with Bonferroni correction. **P* < 0.05 compared to control groups

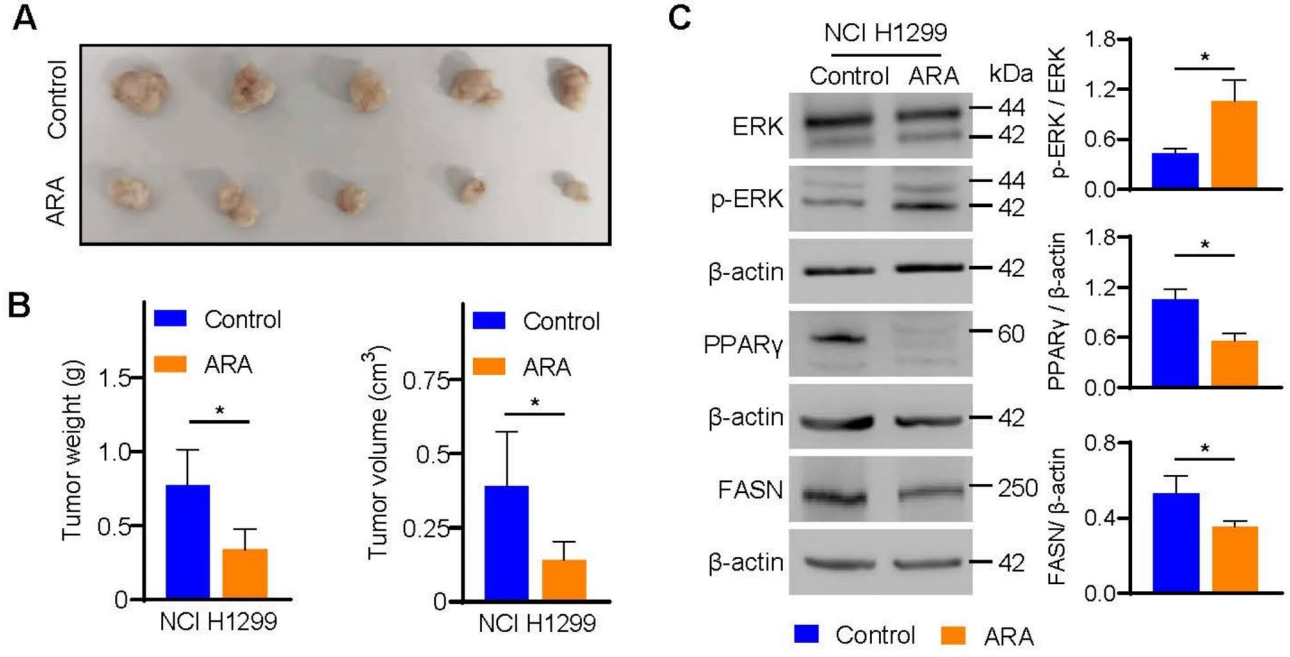

Fig. 6 ARA inhibits tumor growth and modulates the ERK/PPARγ signaling pathway in a lung cancer mouse model. (**A**) Representative image of tumors harvested from the control and ARA-treated groups. *N* = 5. (**B**) Quantification of tumor weight and tumor volume in the control and ARA-treated groups. *N* = 5. (**C**) Immunoblotting analysis of key proteins in the ERK/PPARγ signaling pathway in tumors harvested from the ARA-treated and control groups. Quantification of p-ERK/ERK, PPARγ/β-actin, and FASN/β-actin ratios was performed. Data are presented as means ± SD from four independent experiments, and statistical analyses were performed using the Mann-Whitney U test with Bonferroni correction

that inhibits lipid droplet formation [38, 39], was used to treat A549 and NCI-H1299 cells. Consistent with the effects observed following ARA treatment, GW9662 significantly suppressed cell viability and enhanced both cell death and apoptosis. These results provide strong experimental evidence that inhibiting lipid droplet formation directly impairs lung cancer cell viability and promotes apoptosis, supporting the hypothesis that ARA exerts its anti-tumor effects by modulating lipid metabolism.

The investigation of the ERK/PPARγ signaling pathway provided molecular insights into how ARA mediates its effects on lipid metabolism. PPARγ, a nuclear receptor involved in adipocyte differentiation, maintenance, and function, is often upregulated in cancer cells to meet their increased metabolic demands [40]. Similarly, FASN, an enzyme required for fatty acid synthesis, plays a key role in membrane biosynthesis and energy storage in rapidly dividing cells [41, 42]. The increase in ERK phosphorylation, alongside reduced PPARγ and FASN expression, suggests that ARA might impact lipid synthesis and storage pathways, both crucial for cancer cell survival and proliferation. By activating ERK, ARA might reduce the availability of essential lipids, thereby impairing the survival of lung cancer cells. The paradoxical role of ARA as both an essential fatty acid and an inhibitor of lipid droplet might be because the formation lipid droplets are primarily formed through the accumulation of saturated and monounsaturated fatty acids. Lipid droplet formation is closely associated with fatty acid storage and energy reserves, whereas ARA, being a polyunsaturated

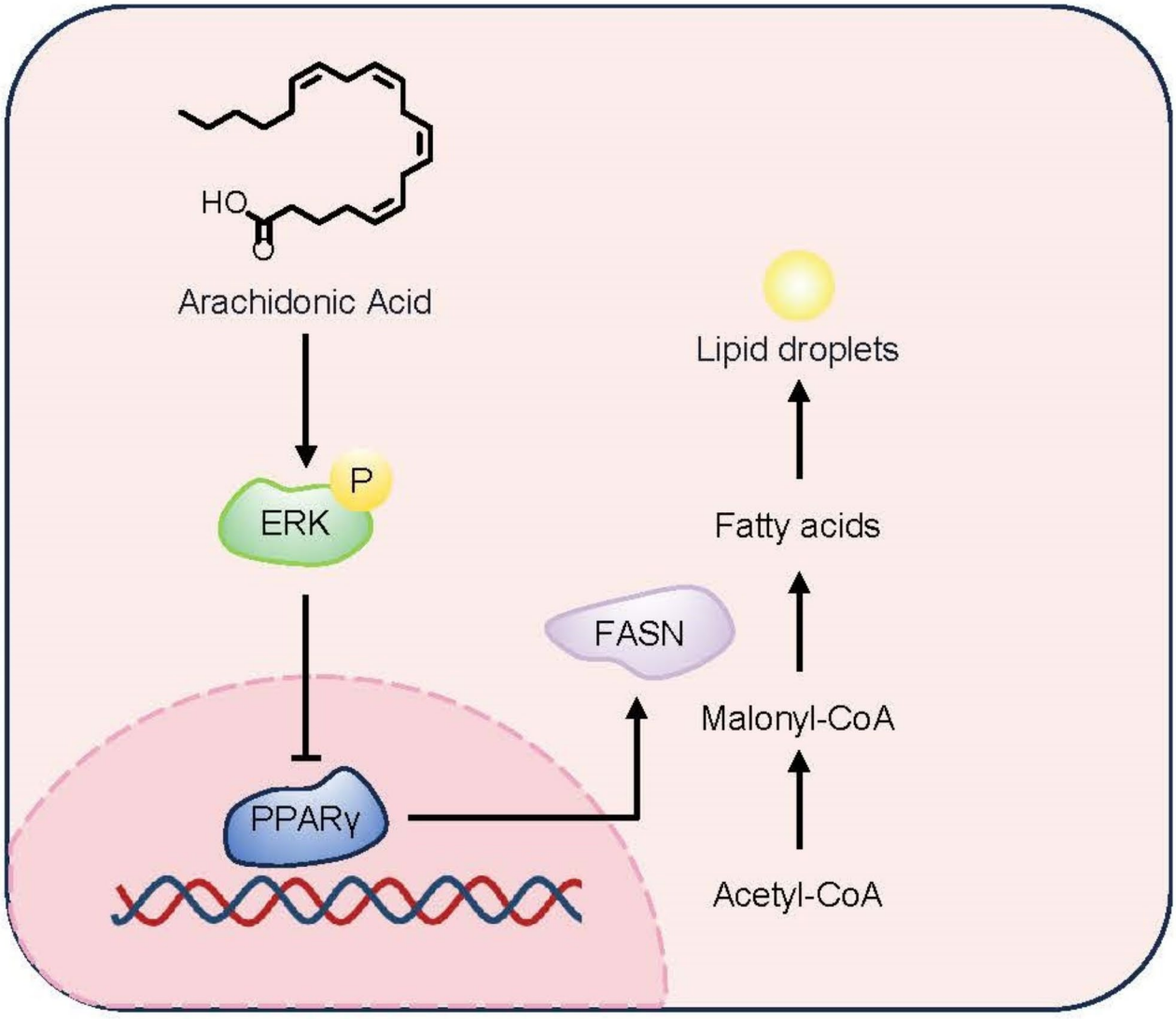

Fig. 7 Schematic representation of the proposed mechanism by which ARA inhibits lipid metabolism through the ERK/PPARγ signaling pathway in lung cancer cells

fatty acid, is mainly involved in the synthesis of phospholipids for cellular membranes rather than energy storage. Furthermore, ARA inhibits key lipid synthesis pathways, including the expression of FASN in this study, reducing the availability of lipids for storage. These actions might disrupt the compensatory balance between lipid ingestion and synthesis, preventing lipid droplet accumulation despite the presence of ARA. In addition to the in vitro findings, the anti-tumor effects of ARA were validated in vivo using a lung cancer mouse model. ARA-treated mice showed a remarkable reduction in tumor size and weight compared to the control group, indicating significant tumor growth inhibition. Consistent with the in vitro mechanism, increased ERK phosphorylation and decreased PPARγ and FASN protein levels were observed in ARA-treated tumors. This suggests that ARA inhibits tumor growth by activating the ERK pathway and suppressing lipid metabolism through downregulation of PPARγ and FASN.

Previous studies have demonstrated that ARA exerts anti-cancer effects through various mechanisms, including lipid peroxidation, oxidative stress induction, and the modulation of key signaling pathways [43]. Among these, lipid peroxidation induced by ARA has been shown to trigger ferroptosis in tumor cells, a process that can be mitigated by antioxidants such as Vitamin E and superoxide dismutase (SOD) [44–47]. This interplay suggests that lipid peroxidation might contribute to the anti-cancer action of ARA, even though this study primarily focuses on the ERK/PPARγ signaling pathway and lipid droplet formation. Moreover, other polyunsaturated fatty acids (PUFAs), such as γ-linolenic acid (GLA), dihomo-γ-linolenic acid (DGLA), eicosapentaenoic acid (EPA), and docosahexaenoic acid (DHA), might affect similar pathways, with varying degrees of potency in cancer inhibition. Comparative studies are needed to determine the most effective PUFA and to delineate shared or distinct mechanisms of action. Additionally, the dual role of ARA as both an essential fatty acid and an inhibitor of lipid droplet formation underscores its unique ability to regulate lipid metabolism and signaling in cancer cells. This highlights its potential as a therapeutic agent. Future research should investigate the precise dynamics of ARA metabolism, its influence on lipid storage, and its broader implications for anti-cancer strategies.

In conclusion, our findings demonstrate that ARA exerts significant anti-tumor effects in lung cancer cells by suppressing cell viability, inducing cell death, and inhibiting colony formation. These effects might be mediated through the ERK/PPARγ signaling pathway and lipid metabolism, as suggested by alterations in key pathway components observed in response to ARA treatment (Fig. 7). However, since no direct functional experiments on lipid metabolism were conducted, further studies are needed to confirm the involvement of lipid metabolism in the anti-tumor mechanism of ARA.

Author contributions

The manuscript was written by LW and XC, with revisions made by LW and JX. Data curation was handled by LW and XC, while XC and JX performed the formal analysis. Project administration was overseen by JX, and XC was responsible for the study design. All authors have given their approval for the final version of the manuscript.

Funding

No funding.

Data availability

No datasets were generated or analysed during the current study.

Declarations

Consent for publication

All the authors read the final version and agree to publish it.

Competing interests

The authors declare no competing interests.

Received: 7 November 2024 / Accepted: 16 February 2025
Published online: 27 March 2025

References

1. Bray F, et al. Global cancer statistics 2022: GLOBOCAN estimates of incidence and mortality worldwide for 36 cancers in 185 countries. CA Cancer J Clin. 2024;74(3):229–63.
2. Nooreldeen R, Bach H. Current and Future Development in Lung Cancer diagnosis. Int J Mol Sci, 2021. 22(16).
3. Hirsch FR, et al. Lung cancer: current therapies and new targeted treatments. Lancet. 2017;389(10066):299–311.
4. Ho GY, Woodward N, Coward JI. Cisplatin versus carboplatin: comparative review of therapeutic management in solid malignancies. Crit Rev Oncol Hematol. 2016;102:37–46.
5. Griesinger F, et al. Efficacy and safety of first-line carboplatin-versus cisplatin-based chemotherapy for non-small cell lung cancer: a meta-analysis. Lung Cancer. 2019;135:196–204.
6. Attili I et al. New generations of tyrosine kinase inhibitors in treating NSCLC with Oncogene Addiction: strengths and limitations. Cancers (Basel), 2023. 15(20).
7. Cooper AJ, Sequist LV, Lin JJ. Third-generation EGFR and ALK inhibitors: mechanisms of resistance and management. Nat Rev Clin Oncol. 2022;19(8):499–514.
8. Liu YQ, et al. Protection against chemotherapy- and radiotherapy-induced side effects: a review based on the mechanisms and therapeutic opportunities of phytochemicals. Phytomedicine. 2021;80:153402.
9. Westover D, et al. Mechanisms of acquired resistance to first- and second-generation EGFR tyrosine kinase inhibitors. Ann Oncol. 2018;29(suppl_1):i10–9.
10. Koulouris A et al. Resistance to TKIs in EGFR-Mutated Non-small Cell Lung Cancer: from mechanisms to new therapeutic strategies. Cancers (Basel), 2022. 14(14).
11. Fan Y, et al. Advances on immune-related adverse events associated with immune checkpoint inhibitors. Front Med. 2021;15(1):33–42.
12. Postow MA, Sidlow R, Hellmann MD. Immune-related adverse events Associated with Immune Checkpoint Blockade. N Engl J Med. 2018;378(2):158–68.
13. Tallima H, El R, Ridi. Arachidonic acid: physiological roles and potential health benefits - a review. J Adv Res. 2018;11:33–41.
14. Panaroni C, et al. Polyunsaturated fatty acid (PUFA) signaling induces ferroptosis-mediated cell-death in multiple myeloma. Blood. 2019;134:3108.
15. Das UN. Tumoricidal action of cis-unsaturated fatty acids and their relationship to free radicals and lipid peroxidation. Cancer Lett. 1991;56(3):235–43.
16. Panaroni C, et al. Arachidonic acid induces ferroptosis-mediated cell-death in multiple myeloma. Blood. 2018;132:4498.

17. Das UN, Madhavi N. Effect of polyunsaturated fatty acids on drug-sensitive and resistant tumor cells in vitro. Lipids Health Dis. 2011;10:159.
18. Zhang N et al. Arachidonic acid regulation of Intracellular Signaling pathways and Target Gene expression in bovine ovarian granulosa cells. Anim (Basel), 2019. 9(6).
19. Jia H, et al. Deciphering the role of fatty acid-metabolizing CYP4F11 in Lung Cancer and its potential as a drug target. Drug Metab Dispos. 2024;52(2):69–79.
20. Kuhn M, et al. STITCH: interaction networks of chemicals and proteins. Nucleic Acids Res. 2008;36(Database issue):D684–8.
21. Gfeller D, et al. SwissTargetPrediction: a web server for target prediction of bioactive small molecules. Nucleic Acids Res. 2014;42(Web Server issue):W32–8.
22. Ru J, et al. TCMSP: a database of systems pharmacology for drug discovery from herbal medicines. J Cheminform. 2014;6:13.
23. Yarla NS, et al. Targeting arachidonic acid pathway by natural products for cancer prevention and therapy. Semin Cancer Biol. 2016;40–41:48–81.
24. Zhao H, et al. Inflammation and tumor progression: signaling pathways and targeted intervention. Signal Transduct Target Ther. 2021;6(1):263.
25. Koundouros N, Poulogiannis G. Reprogramming of fatty acid metabolism in cancer. Br J Cancer. 2020;122(1):4–22.
26. Wang D, Dubois RN. Eicosanoids and cancer. Nat Rev Cancer. 2010;10(3):181–93.
27. Hanahan D, Weinberg RA. Hallmarks of cancer: the next generation. Cell. 2011;144(5):646–74.
28. Vaezi MA, et al. 15-Lipoxygenase and its metabolites in the pathogenesis of breast cancer: a double-edged sword. Lipids Health Dis. 2021;20(1):169.
29. Hanahan D, Weinberg RA. The hallmarks of cancer. Cell. 2000;100(1):57–70.
30. Forgie BN, et al. Vitality, viability, long-term clonogenic survival, cytotoxicity, cytostasis and lethality: what do they mean when testing new investigational oncology drugs? Discov Oncol. 2024;15(1):5.
31. Guo YJ, et al. ERK/MAPK signalling pathway and tumorigenesis. Exp Ther Med. 2020;19(3):1997–2007.
32. Owaki H, et al. Extracellular signal-regulated kinases in T cells: characterization of human ERK1 and ERK2 cDNAs. Biochem Biophys Res Commun. 1992;182(3):1416–22.
33. Zhang W, Liu HT. MAPK signal pathways in the regulation of cell proliferation in mammalian cells. Cell Res. 2002;12(1):9–18.
34. Ren Y, et al. A novel insight into cancer therapy: lipid metabolism in tumor-associated macrophages. Int Immunopharmacol. 2024;135:112319.
35. Fu Y et al. Lipid metabolism in cancer progression and therapeutic strategies. MedComm (2020), 2021. 2(1): pp. 27–59.
36. Wang Z, et al. Lipid metabolism as a target for cancer drug resistance: progress and prospects. Front Pharmacol. 2023;14:1274335.
37. Huang Q, et al. Co-administration of 20(S)-protopanaxatriol (g-PPT) and EGFR-TKI overcomes EGFR-TKI resistance by decreasing SCD1 induced lipid accumulation in non-small cell lung cancer. J Exp Clin Cancer Res. 2019;38(1):129.
38. Xiao J, et al. GW9662 ameliorates nonalcoholic steatohepatitis by inhibiting the PPARgamma/CD36 pathway and altering the gut microbiota. Eur J Pharmacol. 2023;960:176113.
39. Souza-Moreira L, et al. Adipose-derived mesenchymal stromal cells modulate lipid metabolism and lipid Droplet Biogenesis via AKT/mTOR -PPARgamma Signalling in macrophages. Sci Rep. 2019;9(1):20304.
40. Aprile M, et al. PPARgammaDelta5, a naturally Occurring Dominant-negative splice isoform, impairs PPARgamma function and adipocyte differentiation. Cell Rep. 2018;25(6):1577–e15926.
41. Gunenc AN, et al. Fatty acid synthase: structure, function, and Regulation. Subcell Biochem. 2022;99:1–33.
42. Jensen-Urstad AP, Semenkovich CF. Fatty acid synthase and liver triglyceride metabolism: housekeeper or messenger? Biochim Biophys Acta. 2012;1821(5):747–53.
43. Wang B, et al. Metabolism pathways of arachidonic acids: mechanisms and potential therapeutic targets. Signal Transduct Target Ther. 2021;6(1):94.
44. Chen Q, Galleano M, Cederbaum AI. Cytotoxicity and apoptosis produced by arachidonic acid in HepG2 cells overexpressing human cytochrome P-4502E1. Alcohol Clin Exp Res. 1998;22(4):782–4.
45. Lee JY, et al. Polyunsaturated fatty acid biosynthesis pathway determines ferroptosis sensitivity in gastric cancer. Proc Natl Acad Sci U S A. 2020;117(51):32433–42.
46. Mu Y, et al. Activation of pyroptosis and ferroptosis is involved in the hepatotoxicity induced by polystyrene microplastics in mice. Chemosphere. 2022;291(Pt 2):132944.
47. Weitberg AB. Effects of inhibitors of arachidonic acid metabolism and vitamin E on oxygen radical-induced sister chromatid exchanges. Carcinogenesis. 1987;8(11):1619–20.

Publisher's note